

A comprehensive exploration of structural and electronic properties of Molybdenum clusters

Yao Wei¹ and Lev Kantorovich^{1, *}

¹*Theory and Simulation of Condensed Matter (TSCM),
King's College London, Strand, London WC2R 2LS, United Kingdom*

Molybdenum clusters, characterised by their unique structure and intriguing catalytic properties, have gained significant attention in recent years. In several existing studies density functional theory (DFT) methods have been used to find the lowest energy Mo clusters and explore their electronic and magnetic structure. In all cases, with the exception of a single recent study, where a genetic algorithm was employed, initial geometries of the clusters, prior to geometry optimisation, were chosen using heuristic approaches based on symmetry considerations and known structures. DFT calculations were performed using different types of pseudopotentials, from hard to soft, and different types of basis sets. However, no comprehensive study has yet been done in which a DFT method with the best control on its precision would be complemented by a reliable global minimum search method to find the lowest energy Mo clusters. In this work, we employ a combination of a plane wave-based DFT method and *ab initio* random structure searching (AIRSS) technique to find the lowest energy clusters of up to 10 Mo atoms. In each case, the search has been performed for clusters with different spin multiplicities, which enabled us to explore their magnetic structure. The results are compared for both hard and soft pseudopotentials stressing the importance of treating more electrons explicitly, in agreement with some of the previous studies. For most of the low-energy magnetic structures found, we investigate the distribution of their spin densities, and for all low energy clusters, we confirm their stability by calculating their phonon structure. Finally, free energies of the Mo clusters, within the quasi-harmonic approximation, are also calculated and discussed.

I. INTRODUCTION

Adsorption and catalysis play vital roles in the fields of physics and chemistry. Transition metal (TM) clusters, particularly Molybdenum (Mo) clusters, have demonstrated great potential as adsorbents for removing heavy metal ions, organic pollutants, and radioactive nuclides from water [1]. Furthermore, molybdenum exhibits catalytic properties in various processes, including hydrodesulfurization [2], methanol synthesis [3], ammonia synthesis [4], and redox reactions [5]. Additionally, molybdenum serves as an excellent catalyst support, facilitating the preparation of metal or non-metal nanoparticles and improving their catalytic activity and stability [6].

Over the last decade or so, Mo clusters have been extensively studied both theoretically [7–17] and experimentally [18–20]. In Ref. [7] density functional theory (DFT) and a plane wave basis set were used to study structural, electronic, and magnetic properties of molybdenum clusters of up to 55 atoms including linear, planar and 3D clusters whenever possible. A hard Mo pseudopotential was used with only $4d^55s^1$ electrons treated explicitly, which resulted in clusters showing a strong tendency to dimerisation. In [9] a localised basis set and a hard pseudopotential were also used confirming the dimerisation phenomenon in some of the clusters. A localised basis set was also used in [13] where an adsorption of N_2 molecule on the clusters was considered. In

all studies performed with the hard pseudopotential, the lowest energy clusters demonstrated low symmetry (distorted triangles, pyramids, etc.). For each number n of the Mo atoms in the clusters Mo_n , several isomers were found with close binding energies. Moreover, the binding energy and the average bond length demonstrate an oscillating even/odd behaviour as a function of n .

In [12] 4s and 4p semi-core states were included explicitly in the plane wave DFT framework proving the importance of employing a soft pseudopotential in the description of small Mo clusters; in particular, it was demonstrated that the dimerisation tendency between Mo atoms is drastically reduced. This conclusion of the dimerisation effect being an artefact of using hard core pseudopotential on Mo atoms in Mo_n clusters with $n = 2 - 10$ was confirmed in a local basis set simulations [14] where $4s^24p^6$ electrons on each Mo were also included in the treatment explicitly. Some of the clusters became more symmetric; several isomers within 60 meV/atom were found for each value of n . Moreover, atomisation energies demonstrated a monotonic increase with n . They also found that only Mo_3 , Mo_8 and Mo_{10} are magnetic (triplet, quintet and triplet), while all other lowest energy clusters were singlet. In [10] only $4p^6$ electrons were additionally included into a plane wave calculation (alongside the $4d^55s^1$ electrons), with the main emphasis given to studying Mo_nS clusters. A numeric atom-centred atomic basis was used within a scalar-relativistic approach in [16] where a wide range of 3d, 4d and 5d transition-metal clusters were studied including Mo clusters Mo_n with $n = 2 - 10$. It is not clear, however, which electrons were treated explicitly in these calcu-

* lev.kantorovitch@kcl.ac.uk

lations. Average bond distances, effective coordination numbers, binding energies, magnetic and other properties were reported. In [17] Mo, Pt and Mo/Pt clusters were considered using a localised basis set; scalar-relativistic effects were included indirectly via the Mo pseudopotential (unfortunately, no information was provided on that pseudopotential). In this work, the stability of the structures found was checked by calculating clusters' vibrations.

In all research mentioned so far, Mo clusters were chosen by considering various initial geometries with different symmetry including linear, planar and 3D geometries, from both a large set of representative structures as well as those obtained previously; in addition, when preparing initial geometries, distorted versions of known and/or symmetric clusters were also tried. Only recently [8, 11] a more systematic approach based on a genetic algorithm with mutations and mating [21] was employed for the global minimum energy search (for clusters with $n = 2 - 10$) using a DFT method. In this work a localised basis set was used; however, no information was provided on the type of the pseudopotential employed. The authors confirmed previously found structures and discovered a few new ones admitting that depending on the method used the actual structures reported in the literature may differ; they found that from $n = 4$ the lowest energy structures correspond to low symmetry. A number of properties were reported including binding energy, symmetry, average coordinate number, second energy difference, and energy (HOMO-LUMO) gap.

Even though in [8, 11] a genetic algorithm was used to explore the coordinate space of the clusters, a localised basis set was used, and hence it is difficult to verify its convergence, while a plane wave basis set can be easily extended and brought to convergence. Also, only in a few papers the obtained clusters were checked on their stability by calculating their vibrations. Moreover, we did not find any discussion of the spin structure of Mo singlet and non-singlet clusters apart from the reported value of their spin multiplicity; the actual distribution of the spin density is not normally discussed. As far as we are aware, in all calculations reported so far, the van der Waals (vdW) interaction [22] was also not accounted for.

To address these issues, we present here a systematic study of Mo clusters with $n = 2 - 10$ using a plane wave DFT method with both hard and soft pseudopotentials and high energy cutoff. In all calculations, a vdW correction to the total energy was added. For each value of n , spin multiplicities $M = 2S + 1$ of up to 7 were considered individually to find all clusters with the binding energies within a 1.0 eV threshold, so that all clusters MO_n within that threshold across all considered spin multiplicities could be predicted. To generate initial structures prior to their geometry optimisation, we employed an *ab initio* random structure searching technique that with high probability enabled us to obtain the lowest energy structures for each spin multiplicity (the 'putative' global minimum). All the atomic positions of the global min-

imum configurations and those close to them in energy isomers obtained in this study are reported in Supplementary Information. The stability of each structure is confirmed by a comprehensive vibrational analysis, and in each spin-polarised case, the distribution of the spin density is also given. The obtained lowest-energy structures are compared with those reported in the literature.

The plan of the paper is as follows. In the next Section, we discuss our computational method. In Section III results are considered. Finally, in Section IV conclusions are drawn.

II. COMPUTATIONAL METHODS

For each number of Mo atoms n in the cluster, several values of the spin multiplicity $M = 2S + 1$ were considered, where $S = \frac{1}{2}N_{ud}$ is the total spin with N_{ud} being the difference in the numbers of the electrons of both directions of the spin. In this study, we limited ourselves to the values of $M = 1, 3, 5, 7$ only (correspondingly, $N_{ud} = 0, 2, 4, 6$). Higher values of M are considered unlikely even for clusters with large n . A significant set of several hundreds of initial structures was chosen, for each value of n and M , using a random structure search package AIRSS (Atomic and Ionic Relaxation from Structure Searching) [23, 24] that is designed to explore the configurational space in order to find the lowest energy Mo clusters. The initial structures were selected by defining various physical conditions such as atomic distance, symmetry, element composition, element ratio, etc. The software performs a search through the configurational space to identify promising atomic structures.

Once the potential structures are identified, VASP (Vienna Ab initio Simulation Package) [25] is employed to perform structural geometry relaxation of each candidate structure and compute its binding energies (see below). The structures obtained are then compared with each other to select distinct structures. We used sufficiently large unit cells in each case to prevent clusters from interacting with their images, and correspondingly the Γ point \mathbf{k} -point sampling was only employed. This allows benefiting from a faster implementation in VASP, specifically designed to deal with real wavefunctions. This is particularly advantageous when dealing with a large number of structures required for high-throughput AIRSS searches.

The local structural relaxations and total energy calculations were performed within a DFT framework using the Perdew, Burke, and Ernzerhof (PBE) generalised gradient approximation (GGA) functional [26]. Additionally, the van der Waals (vdW) dispersion correction was introduced employing the Grimme-3 method [27, 28], and electron-ion interactions were described using projector-augmented wave (PAW) pseudopotentials [29].

Two types of pseudopotentials are compared: a hard core Mo pseudopotential that only treats explicitly $4d^55s^1$ valence electrons on each Mo atom, and a soft Mo pseudopotential under which $4s^24p^64d^55s^1$ electrons

are considered explicitly. A plane-wave kinetic-energy cutoff of 300 eV was used, and each relaxation calculation was considered finished when the energy threshold of 10^{-5} eV was reached, while the atomic forces were not larger than 0.01 eV/Å. To assess the accuracy of the calculations, the optimisation of Mo₂ was performed. The computed bond lengths (1.931 Å) and bond energy (1.973 eV/atom) closely match the experimental findings (bond length: 1.93~1.94 Å and bond energy: 2.06 ± 0.38 eV/atom [30–32]) when utilising the soft Mo pseudopotential, see the comparison in Table I. However, the calculated bond lengths (1.700 Å) and bond energy (3.104 eV/atom) do not align well with the experimental outcomes when employing a hard pseudopotential that considers explicitly only $4d^55s^1$ valence electrons.

The binding energy of a Mo_n cluster is defined in the usual way as

$$E_b = \frac{1}{n} (nE_1 - E_n), \quad (1)$$

where E_1 is the total energy of a single Mo atom and E_n is the total energy of the cluster of n Mo atoms.

All calculations were performed using spin-polarisation and by fixing the number of spin-up and spin-down electrons, even if these two numbers were the same ($M = 1$). The spin density $s(\mathbf{r}) = \rho_\uparrow(\mathbf{r}) - \rho_\downarrow(\mathbf{r})$ is defined as a difference of the electronic densities of either of the spins. When integrated over the whole space of the cluster, it gives the number N_{ud} of the electrons with unpaired spins. To preview the spin density, we used VASPKIT [33] for DFT output post-processing and VESTA [34] for visualisation.

For each cluster obtained using AIRSS an additional geometry relaxation was performed with more stringent relaxation criteria (the maximum atomic force 0.01 eV/atom) prior to running the vibrational calculations. The latter calculations were performed using finite differences (the frozen-phonon method) as implemented in the VASP code.

To calculate the (Helmholtz) free energy of the clusters, we used the quasi-harmonic approximation [35] with the free energy approximated by

$$F = E_{DFT} + \sum_{i=1}^{3n-6} \left[\frac{\hbar\omega_i}{2} + k_B T \ln(1 - e^{-\beta\hbar\omega_i}) \right], \quad (2)$$

where E_{DFT} is the DFT total energy and the second term accounts for the contribution from atomic vibrations. There, we sum over all vibrational frequencies ω_i excluding rotations and translations (there are exactly six of these to be excluded in all cases considered below as linear clusters have far lower binding energies than non-linear ones [36] and have been excluded from the very beginning). The first term within the square brackets is zero-point vibrational energy, while the second term comes from taking into account the possibility for the phonons to be excited; k_B is the Boltzmann constant and

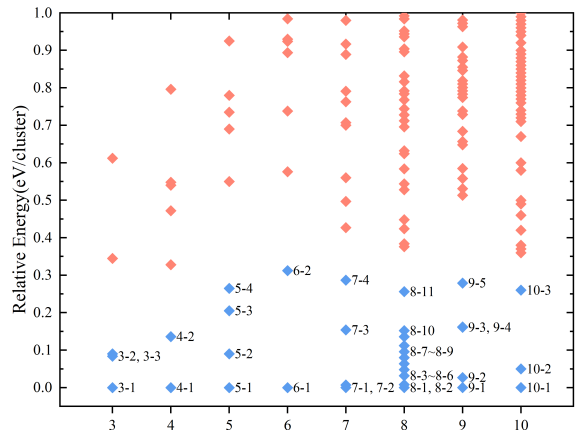


FIG. 1. Energies (in eV) of DFT relaxed Mo clusters containing between $n = 3$ and $n = 10$ Mo atoms are shown. For each n the energies are given relative to the cluster with the lowest energy (indicated as having 0.0 energy). The clusters are numbered according to the notations adopted in Table II, and for most of the clusters their point group symbol is also given. The clusters with the lowest energies that are considered in ore detail in this work are shown using red diamonds; others are indicated by black diamonds.

T absolute temperature. Six frequencies appear in these calculations as having either very small positive and/or imaginary values and were easily eliminated; this step was also verified by previewing the corresponding normal modes using the Interactive phonon visualiser tool [37] and making sure that the eliminated modes correspond to either a translation or rotation of the whole cluster.

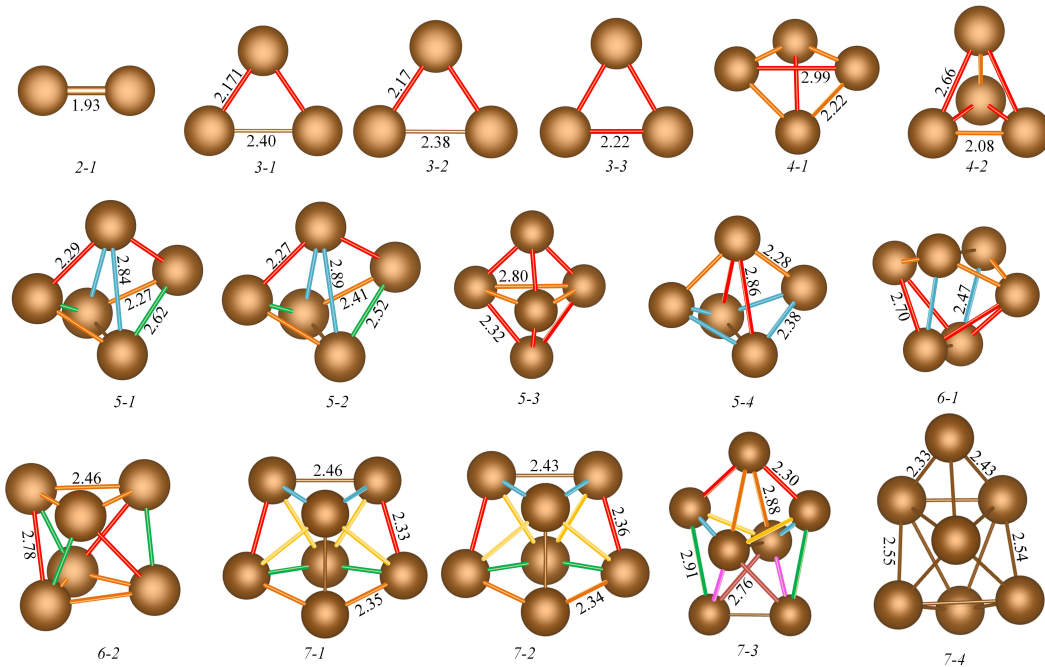
III. RESULTS

We have used the DFT method and the AIRSS code to find the lowest energy Mo clusters of different multiplicities with the number of Mo atoms n ranging between 2 and 10.

To initiate our discussion, we first would like to show, for each n , all structures we have found that are within, say, 1.0 eV in their binding energy from the lowest energy structure. Figure 1 illustrates this. The energy of the structure with the lowest energy for any given value of n is defined as 0. One can see that the number of structures we found could be in some cases very large. Three points can be stressed here. First of all, we see that in some cases ($n = 3 - 7$) there is a relatively small number of clusters close in energy to the best structure (within 1.0 eV).; in other cases ($n = 8 - 10$) the number of clusters within this energy range is much larger (41, 36, and 64, respectively). Secondly, for $n = 3 - 6$, 10 there is a clear energy gap between the lowest energy structure and the next one; in the cases of $n = 7 - 9$, there is a very small energy difference between the best

	bond length (Å)	bond energy (eV/atom)
experiment [30–32]	1.93~1.94	2.06 ± 0.38
this paper $4s^2 4p^6 4d^5 5s^1$	1.931	1.973
this paper $4d^5 5s^1$	1.700	3.104

TABLE I. The comparison of two pseudopotentials for a cluster with two atoms

FIG. 2. The lowest energy clusters for $n = 2 - 7$ labeled as in Tables II and III are shown. We also show the interatomic distances (in Å); equal distances (within a tolerance of about 0.01 Å) are shown, for each cluster, with the same colour.

energy structures. Note, however, that these lowest energy clusters may not have the same multiplicity as is clear from Tables II–V. Furthermore, it is evident that as the number of atoms in the clusters increases, there is a gradual expansion in the variety of structure types that have energies within 1.0 eV relative to the lowest energy structure.

These observations underscore the importance of conducting comprehensive and systematic structure searches as in many cases there are structures very close in energy and hence of a similar likelihood to exist and be observed.

Results of DFT calculations corresponding to the zero temperature will be discussed first. Only the lowest energy structures are considered in detail here. These are indicated in Fig. 1 using blue diamonds; other structures, not discussed here in detail, are indicated by red diamonds. The geometries of all blue structures are given in the Supporting Information. For each value of n , the lowest energy structure and a few structures with closest energies for different multiplicities considered below in detail are shown in Figs. 2 and 3. More detailed information about these structures is collected in Tables II–V. Below we shall consider each case of the number of Mo atoms n separately, starting from $n = 3$.

A. Lowest energy Mo clusters

Before we discuss in detail the Mo atom clusters we have found, a note is in order concerning difficulties we have encountered when trying to compare our structures with those reported in this literature. We provide in the Supporting Information atomic positions of all high binding energy structures and describe their symmetry in detail. However, with a single exception of Ref [16], in all cases geometries reported in the literature are not given explicitly via atomic positions; only pictures of the relaxed structures were given with point groups and some interatomic distances. Hence, a precise comparison cannot be made; hence, in doing so below we have tried our best employing all the information available.

1. $n = 3$

We have found 5 isomers with the energies within 1 eV from the lowest energy structure. Three lowest structures are shown in Fig. 2 and their characteristics are given in Table II. Remarkably, the highest stability cluster labelled 3-1 is the one with the planar geometry of an

Cluster label	1-1	2-1	3-1	3-2	3-3	4-1	4-2	5-1	5-2	5-3	5-4
Multiplicity	7	1	3	1	3	1	1	1	3	1	3
Binding energy	(-4.648)	1.973	2.184	2.156	2.154	2.734	2.700	3.069	3.050	3.028	3.016
Symmetry group		$D_{h\infty}$	C_{2v}	C_{2v}	D_{3h}	D_{2d}	D_{2d}	C_2	C_2	D_{3h}	C_{2v}

TABLE II. Clusters' labels, multiplicities, binding energies (per atom, in eV), and symmetry groups of all lowest energy clusters corresponding to $n = 2 - 5$. Note that for $n = 1$ we give the total energy of the Mo atom.

Cluster label	6-1	6-2	7-1	7-2	7-3	7-4
Multiplicity	1	3	3	1	1	1
Binding energy	3.423	3.371	3.562	3.561	3.537	3.517
Symmetry group	C_{2v}	D_3	C_s	C_s	C_2	C_1

TABLE III. Clusters' labels, multiplicities, binding energies (per atom, in eV), and symmetry groups of all lowest energy clusters corresponding to $n = 6, 7$.

isosceles triangle having C_{2v} point symmetry. The length of the two short sides of this configuration measures 2.171 Å, the longest side is 2.397 Å and the multiplicity $M = 3$, with a binding energy of 2.184 eV/atom. Interestingly, the structure 3-3 corresponding to the equilateral triangle has a lower binding energy by 0.03 eV. It has the same multiplicity and similar bond length. Our results somewhat contradict the previous results of Refs. [9, 12, 17], which predicted the lowest energy structure to be also of an isosceles triangle, but with two isosceles sides longer than the base. The studies [8, 13] claimed instead that the equilateral triangle structure is the most stable, at variance with our results; this is most likely to do with the localised basis set used in these studies and a hard pseudopotential (that is not specified). However, our results generally agree with those in Ref. [7, 10, 14, 16] where a similar soft pseudopotential was used.

In addition to the previously discussed structures, there is also another structure labelled 3-2. The geometry of the structure 3-2 is similar to 3-1, but it has different Mo-Mo distances and multiplicity. The binding energy of 3-3 is by 0.002 eV lower than that of 3-2.

The three lowest energy structures, as having almost identical energies (the energy differences are smaller than the precision of DFT), are all equally likely and hence all have to be accounted for in any Mo clusters studies.

A notable observation is that the energy associated with a linear three-atom arrangement (not shown) is elevated by approximately 1 eV per atom compared to that of the best triangular arrangement discussed above.

2. $n = 4$

There are seven isomers whose energies lie within 1 eV from the lowest energy structure, two of them are analysed in detail in Fig. 2 and Table II. Notably, these two structures share common traits, including the same multiplicity $M = 1$ (and no spin polarisation) and the (rather high) D_{2d} point group symmetry. The 4-1 structure has the lowest energy, featuring a tetrahedral-like configura-

tion characterised by four equally short edges measuring 2.22 Å, complemented by two extended edges of 2.99 Å, with the binding energy of 2.734 eV/atom. On the other hand, the structure labelled 4-2 is by 0.034 eV lower in the binding energy compared to the former structure and adopts closer to a triangular pyramid configuration with two sides being equal to 2.66 Å and two other sides being shorter (2.08 Å).

Both our geometries are of high symmetry which contradicts the result found in [8] whose best structure has no symmetry; their best structure also has a different multiplicity ($M = 3$) to ours. Our best structure is also quite different from the one found in [10, 16, 17]: in [16, 17] the same symmetry D_{2d} is reported and the multiplicity; however, their structure is nearly flat; at the same time, the cluster found in [10] has a lower C_{2v} symmetry and also looks rather flat as compared to ours.

We exclude other structures from our discussion due to energy disparity from the second lowest energy structure of at least 0.2 eV.

3. $n = 5$

There are 9 isomers found in this case whose energies are within 1 eV range from the lowest energy structure. Four lowest energy configurations are shown in Fig. 2 and their characteristics are given in Table II. The structure labelled 5-1 stands out with the highest binding energy of 3.069 eV/atom exhibiting the C_2 symmetry (with the second order axis passing vertically through the uppermost atom) and multiplicity $M=1$ (no spin polarisation). The following next in energy structure 5-2 has the second-highest binding energy of 3.050 eV/atom, and is of the same symmetry; however, its multiplicity is 3 with slightly different Mo-Mo distances as indicated in Fig. 2. The structure labelled 5-3 presents D_{3h} point symmetry, with the third order axis passing vertically through the top and the bottom atoms; six of nine bonds of the structure have the same length of 2.32 Å, its configuration consists of two regular triangular pyramids stacked together. The structure labelled 5-4 possesses a lower

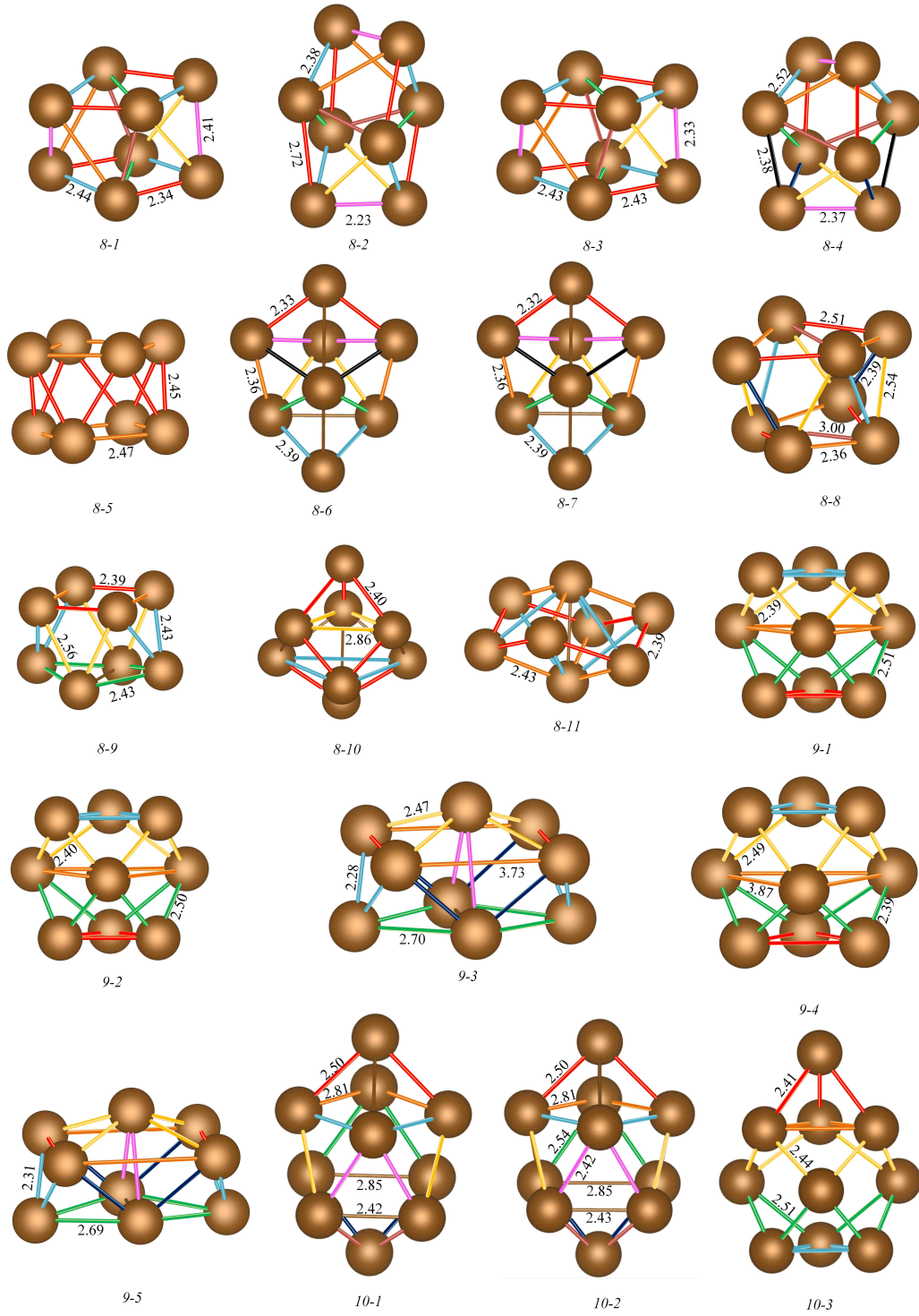


FIG. 3. The lowest energy clusters for $n = 8 - 10$ labeled as in Tables IV and V. We also show some of the interatomic distances (in Å) with equal distances (within a tolerance of about 0.01 \AA) being shown with the same colour.

binding energy with multiplicity $M=3$ and C_{2v} symmetry, the second order axis going vertically through the upper atom. Despite the differences in the symmetry between these four configurations, their appearances closely resemble one another.

Our best structure 5-1 agrees well with the cluster found in [16, 17] both by the multiplicity and symmetry. However, the cluster reported in [10] has higher symmetry C_{2v} and a different multiplicity ($M = 3$). Also, no symmetry for their best five atom cluster was reported

in [8] which is at variance with our results.

4. $n = 6$

There are 8 isomers whose energies lie within 1 eV from the lowest energy structure, 6-1. Two lowest energy configurations are shown in Fig. 2 and Table III. The binding energy of 6-1 is 3.423 eV/atom, it exhibits the C_{2v} symmetry with the second order axis passing through the middle points of the upper and lower dimers; its multiplicity is $M = 1$ (no spin polarisation). 6-2 has higher symmetry D_3 with its upper and lower three atoms forming parallel equilateral triangles (the lower triangle being somewhat rotated with respect to the upper one); the third order axis goes vertically through the centres of both triangles. Its multiplicity is $M = 3$. There is a notable energy gap of more than 0.3 eV between the structure 6-1 and the subsequent second-lowest energy structure 6-2.

The most stable structures of six Mo atoms reported in [10, 16, 17] have C_{2v} symmetry and $M = 1$ in agreement with our best structure 6-1. However, no symmetry was reported in [8], although their multiplicity is the same as ours.

5. $n = 7$

We have found 14 isomers whose energies are within the 1 eV range from the lowest energy structure. Four lowest energy configurations are shown in Fig. 2 and Table III. The structure labelled 7-1 has the highest binding energy of 3.562 eV/atom exhibiting the C_s symmetry (with the symmetry plane passing vertically through the three atoms in the middle) with multiplicity $M = 3$. The structure labelled 7-2 has similar symmetry and interatomic distances; however, its multiplicity $M = 1$ is different; it exhibits a slightly higher energy compared to the previous one. As for the remaining two structures of the lowest energy, namely 7-3 and 7-4, the symmetry of 7-3 is C_2 with the second order axis passing through the upper atom vertically down through the middle points of the other three pairs of atoms, each pair of atoms having the same vertical coordinate, while 7-4 may seem to have C_s symmetry if to be judged by an eye, although a careful analysis confirms that there is no symmetry. Structures 7-2, 7-3 and 7-4 have nearly identical binding energies and multiplicity; however, their geometries are in fact quite different.

We have found our structure 7-1 looking similar and of the same symmetry C_s as in [10, 16], although the multiplicity in [16] is different to ours. The same multiplicity $M = 3$ is found in [8]; however, they report no symmetry in their cluster. The best structure found in [17] is of the same symmetry and multiplicity, although it looks very different.

6. $n = 8$

A total of 41 isomers fall within the 1 eV energy range of the lowest energy structure. In Figure 3, we present 11 lowest energy configurations, and their characteristics can be found in Table IV. Interestingly, unlike clusters composed of 2 to 7 atoms, eight-atom clusters demonstrate a significant diversification in structural options. In this work, we focus on structures within a narrow energy range of 0.2 electron volts, as they are of particular interest (the next set of clusters are worse at least by 0.1 eV in their binding energies).

Configuration 8-1 has the highest binding energy of 3.714 eV/atom exhibiting the D_2 symmetry with multiplicity $M = 5$. Eight atoms of this cluster split into two 4-atom sets lying in two parallel planes; one second order axis of the D_2 point group passes vertically through the centres of the two quadrilaterals; two other perpendicular second order axes, perpendicular to the former one, pass within the plane located midway between the two planes of the quadrilaterals. Compared to 8-1, structures 8-3 and 8-8 have similar symmetry, interatomic distances and binding energies; however, all three clusters have different multiplicities and hence electronic structures. 8-2 and 8-4 also share the same symmetry, C_2 this time, with the 2nd order axis passing vertically through the middle points of the pairs of upper and lower atoms. 8-5 may look similar to 8-1 or 8-3; however, it has higher symmetry D_{4d} : the two parallel quadrilaterals are perfect squares placed symmetrically on top of each other and rotated by 45° around the vertical C_4 axis passing through the centres of the two squares. 8-6 and 8-7 have almost identical geometry corresponding to the group C_s ; the only mirror plane passes through the four atoms arranged vertically on the picture. 8-9 is somewhat similar to 8-5: there are two quadrilaterals formed by the four upper and four lower atoms; however, only the lower 4 atoms form a square, the upper 4 atoms actually form a parallelogram reducing the symmetry to C_{2v} . Cluster 8-10 has the highest T_d symmetry with one of the third order axes passing vertically through the upper and lower atoms; it is only by 0.126 eV lower in binding energy than the lowest energy structure 8-1. Finally, structure 8-11 possesses high D_{3d} symmetry with the third order axis passing vertically through the upper and lower atoms.

Compared to available literature, our structure 8-1 looks similar to the one reported in [10] although their structure has different multiplicity and much higher symmetry D_{4d} . In fact, their structure is comparable with ours 8-5 both in symmetry and multiplicity. Lower symmetry clusters (and also looking rather different) were reported in [8, 16]; they also have a different multiplicity to ours. One may however find some similarities of their clusters to ours of lower energy. The cluster found in the recent study [17] looks similar, but is of much lower symmetry C_2 ; it also has different multiplicity to ours.

Cluster label	8-1	8-2	8-3	8-4	8-5	8-6	8-7	8-8	8-9	8-10	8-11
Multiplicity	5	1	3	3	1	3	1	1	1	1	1
Binding energy	3.714	3.710	3.709	3.709	3.709	3.705	3.700	3.697	3.697	3.693	3.682
Symmetry group	D_2	C_2	D_2	C_2	D_{4d}	C_s	C_s	D_2	C_{2v}	T_d	D_{3d}

TABLE IV. Clusters' labels, multiplicities, binding energies (per atom, in eV), and symmetry groups of all lowest energy clusters corresponding to $n = 8$.

Cluster label	9-1	9-2	9-3	9-4	9-5	10-1	10-2	10-3
Multiplicity	3	1	1	5	3	3	1	1
Binding energy	3.853	3.850	3.835	3.835	3.814	3.923	3.918	3.897
Symmetry group	D_{3h}	D_{3h}	C_{2v}	D_{3h}	C_{2v}	C_s	C_s	C_{3v}

TABLE V. Clusters' labels, multiplicities, binding energies (per atom, in eV), and symmetry groups of all lowest energy clusters corresponding to $n = 9, 10$.

7. $n = 9$

We have identified 36 isomers with energies falling within the 1 eV range of the lowest energy structure. A considerable energy gap becomes apparent between the fifth and sixth lowest energy configurations. In Figure 3 our investigation will be concentrated on the five lowest energy structures, and their characteristics can be found in Table V.

Structures 9-1, 9-2, and 9-4 display remarkable similarities and are very close in their energies (per atom). They have D_{3h} point group symmetry with the third order axis passing vertically through the centres of the two equilateral triangles formed by the three upper and three lower atoms. All three structures have different multiplicities, however. Yet again we observe geometrically almost identical structures and of practically the same energies (9-4 is only lower by 0.162 eV from 9-1), but with remarkably different electronic structures. Next, 9-3 and 9-5 look similar and have the same C_{2v} symmetry formed in the following way: there are four atoms at the bottom in a form of a rhombus; four atoms above them form a rectangular; the ninth atom above them is placed along the vertical second order axis that passes through the centres of both quadrilaterals. In spite of almost identical geometry, the two clusters have different multiplicities.

Our best structure has a higher symmetry than reported in Refs. [8, 10, 16]: their clusters do not have a third order axis at all. The best cluster in [16] resembles our structure 9-3, both in symmetry and multiplicity; the cluster in [10] looks similar to ours 9-1 and has the same multiplicity, but lower symmetry C_{2v} . Only C_s symmetry cluster is reported in [8] of the same multiplicity as ours 9-1. The study [17] reported the C_{3v} symmetry with the third order axis and the same multiplicity as our 9-1; however, their structure looks very different.

8. $n = 10$

In this case, there are 64 isomers whose energies lie within 1 eV from the lowest energy structure, only three configurations exhibiting the lowest energies (see Fig. 1) will be considered in more detail here; they are shown in Fig. 3 and in Table V. 10-1 and 10-2 share the same C_s symmetry and are almost identical in the binding energy (the difference is only 0.05 eV), with the symmetry plane passing through the four atoms forming an imaginary vertical line through the middle of each figure. Their electronic structure is however different: if 10-1 has two unpaired electrons (triplet, $M = 3$), 10-2 is in the singlet state; however, both clusters are spin polarised (Section III C). A more symmetrical 10-3 cluster possesses C_{3v} symmetry with the third order axis passing vertically through the upper atom and the centre of the equilateral triangle formed by the three atoms immediately underneath. Its energy is by 0.21 eV lower than of 10-2; it is not spin-polarised.

The clusters proposed in Refs. [8, 10, 16, 17] have multiplicity $M = 1$ and all look similar: they have four atoms at the top, four at the bottom and two in between; neither of our best structures shown in Fig. 3 has this particular arrangement of atoms. Our best structure 10-1 has a very low C_s symmetry (D_{2h} in [10, 16] and no symmetry in [8]) and multiplicity $M = 3$. However, after carefully examining all the structures we have generated, we found a structure of D_{2h} symmetry and with $M = 1$ that also looks similar to the structure reported in Refs. [8, 10, 16]; note, however, that the binding energy of that structure is by 0.36 eV lower than that of 10-1 and hence was not included in our detailed analysis here.

B. Free energy

In the preceding sections, we presented results of zero-temperature DFT simulations based on structural searches to identify the lowest energy configurations for clusters composed of varying numbers of Mo atoms. No-

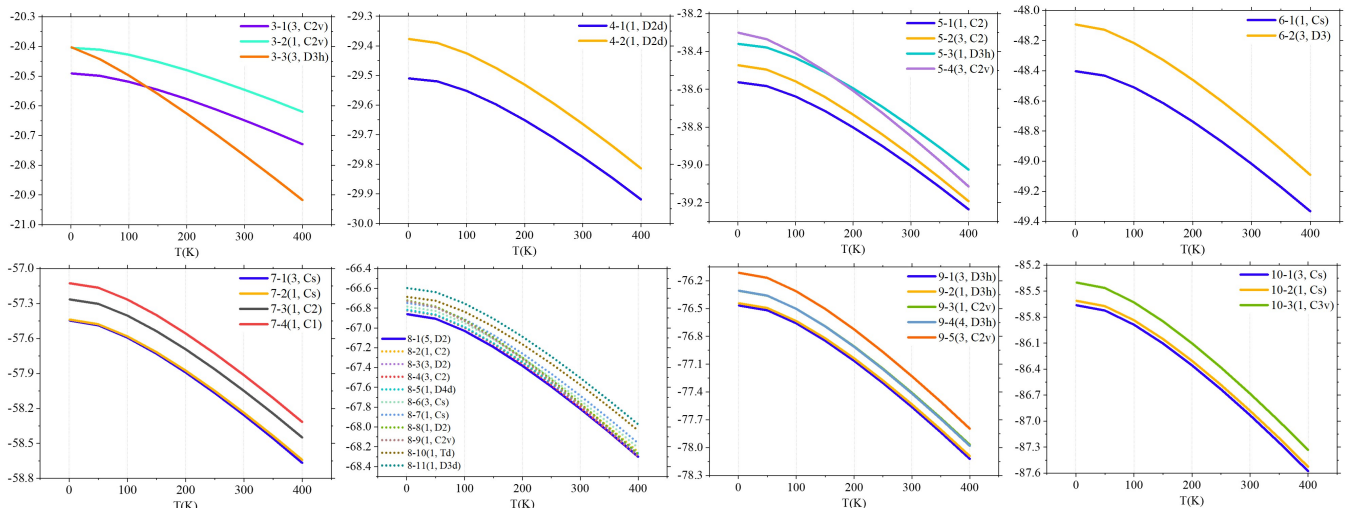


FIG. 4. Free energies of DFT relaxed Mo clusters containing between $n = 3$ and $n = 10$ Mo atoms plotted versus temperature.

tably, our analysis revealed many clusters of close energies (isomers), especially for large values of n . To shed light on the stability of different isomers at higher temperatures, we conducted the calculations of vibrational frequencies for all low-energy structures (marked blue in Fig. 1) and correspondingly worked out their free energies as a function of temperature.

The vibrational frequencies of the clusters are given in the Supporting Information for the soft pseudopotential. First of all, we note that the frequencies are found real in all cases which proves that the obtained geometries reported in Figs. 2 and 3 are stable. The comparison of the vibrational frequencies for the two types of the pseudopotentials was made only for two clusters. We considered clusters 3-3 and 7-1, relaxed using the hard pseudopotential and shown in Fig. S1. Their geometries are similar to the clusters 3-1 and 7-1 obtained using the soft pseudopotential; also, their multiplicities are the same in both cases. However, as can be seen from the comparison in Table S9, the vibrational frequencies in both cases differ considerably.

The calculated free energies for the temperatures of up to 400 K and soft pseudopotentials are shown in Fig. 4. The free energy graphs yielded insightful observations. In all cases, the free energy is going down with the temperature (as expected), and in most cases, the order of the stability of the clusters found at zero temperature does not change. However, there are three notable exceptions found for the cases of $n = 3$, 5 and 8. In the former case, at $T = 0$ cluster 3-1 is lower in energy than 3-2; however, the order of stability of these two clusters is reversed at T around 130 K and after that temperature cluster 3-2 becomes more energetically favourable. In the case of $n = 5$ the stability of the clusters 5-3 and 5-4 swapped at T around 170 K, so that at higher temperatures the clus-

ter 5-4 is more favourable. Finally, in the case of 8 Mo atoms clusters, the lowest energy structure 8-1 remains the most favourable across the whole T range considered; however, free energies of structures 8-2 to 8-8 approach it rather closely, with structures 8-4, 8-5 and 8-8 having the free energy almost the same at $T = 400$ K.

These intriguing observations highlight a subtle interplay in the structural stability of some of the clusters with temperature. The free energy calculations underscore the complex nature of cluster stability and provide valuable contributions to the understanding of Mo atom clusters' thermodynamic behaviour.

C. Spin density

The spin density distributions for clusters showing spin polarisation (some of these have multiplicity $M = 1$) are shown in Fig. 5, and their magnetic moments are shown in Tables II-V.

Note that we specifically checked that most of the clusters with $M = 1$ do not have any spin polarisation even though all calculations, even for this multiplicity, were done with spin polarisation switched on. However, clusters 3-2, 8-7 and 10-2 do have non-zero spin density as can be seen from the Figure: regions of both positive and negative spin density $s(\mathbf{r})$ occupy practically equal regions of space leading to no net spin density overall, $\int s(\mathbf{r})d\mathbf{r} = 0$.

In cluster 3-1 we have $M = 3$ corresponding to two more electrons having spin up; it is seen in the Figure that the excess of the spin-up electrons is localised on the lower two atoms, while the upper atom has excess of spin-down electrons. In 5-4 (also $M = 3$) the excess of the spin up density is localised mostly on the three atoms

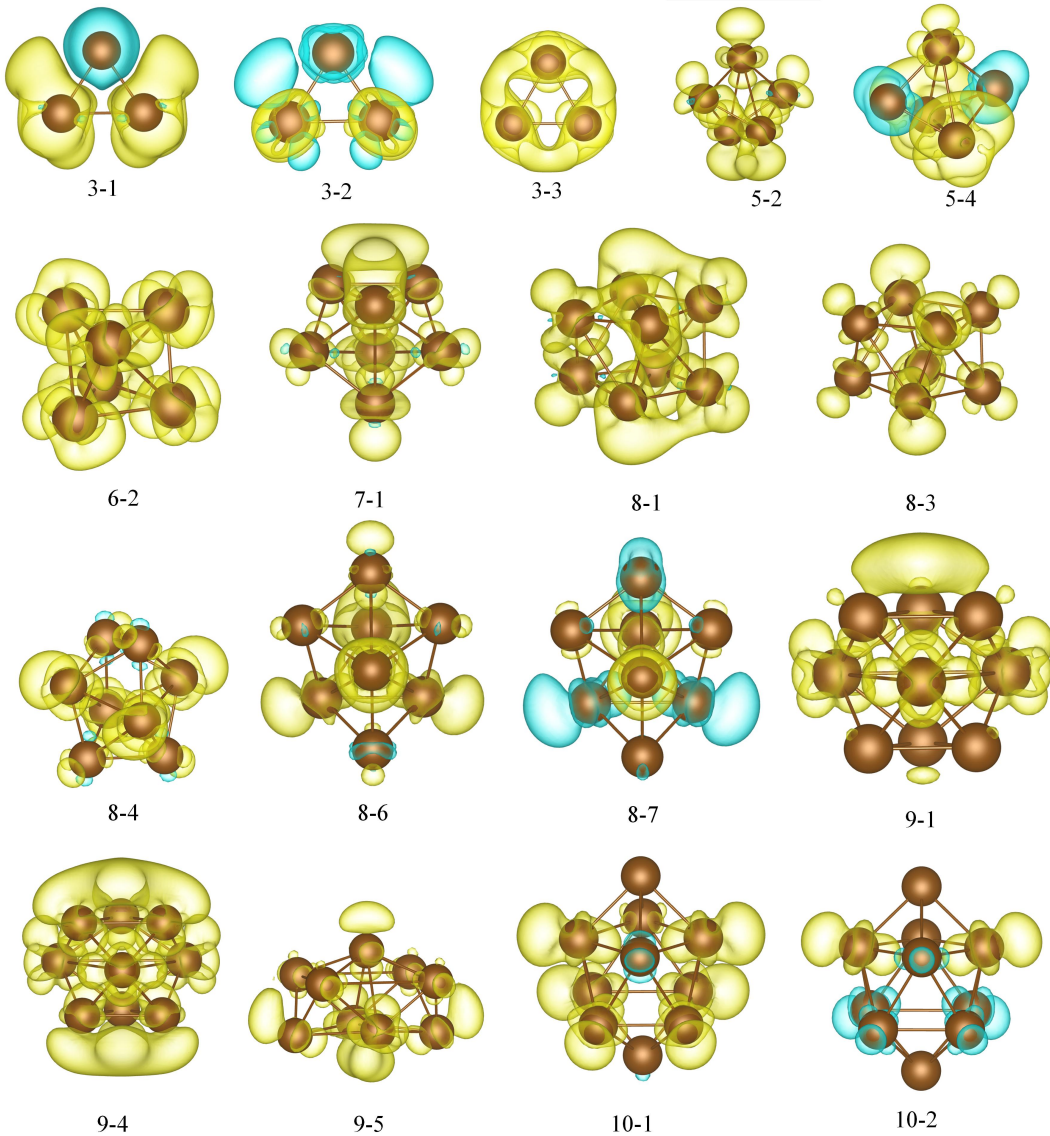


FIG. 5. Spin density of DFT relaxed spin-polarised Mo clusters containing between $n = 3$ and $n = 10$ Mo atoms. Constant value spin density isosurfaces of $\pm 0.003 \text{ \AA}^{-3}$ are shown (yellow and blue correspond to positive and negative values, respectively). The orientations of the clusters are the same as in Figs. 2 and 3.

forming a vertical plane, and there is a localisation of the spin-down density that is distributed over two side atoms. In clusters 3-3, 5-2, 6-2, 7-1, 8-3, 8-4, 8-6, 9-1, 9-5, and 10-1 two unpaired spin-up electrons are distributed over the whole cluster; only small pockets of negative spin density are seen in clusters 5-2, 7-1, 8-4, 8-6, and 10-1, these are not expected to affect appreciably the value of their magnetic moments. In clusters 8-1 and 9-4 we have 4 unpaired spin-up electrons ($M = 5$); their density is distributed over the whole volume of the clusters.

D. Comparison with the hard pseudopotential calculations

We have also performed similar calculations with a hard pseudopotential. The results are collected in the Supporting Information. The geometries of the clusters with lowest energies (the highest binding energies) are shown in Fig. S1. We see, in agreement with previous studies [9], that linear and planar structures are found in this case as being of the lowest energy; in some cases, atoms tend to dimerise (e.g., clusters 4-1, 4-4, 6-2, 9-1, and 9-3). Both of these tendencies contradict our main results given above and are based on calculations with soft pseudopotentials. As was also mentioned in Section III B,

vibrational frequencies of the clusters similar in geometry and multiplicity but obtained with two pseudopotentials, differ considerably. On the whole, we should conclude that the results obtained with hard pseudopotentials could be quite misleading.

IV. CONCLUSIONS

In this work we have presented a comprehensive investigation of Mo clusters with up to $n = 10$ atoms. Using the AIRSS method [23, 24] we obtained a large number of clusters of lowest energies for each value of n . The number of obtained clusters within 1.0 eV from the lowest energy cluster varies with n , with this number quickly growing from 5 for $n = 3$ to 64 for $n = 10$. In each case of n for clusters with energies close to the lowest one, we have given a detailed description of the clusters' symmetry and provided their atomic positions and spin densities. Some of our results agree with the clusters found by other researchers, both by their symmetry (either exactly or very close) and multiplicity, in a few cases new clusters were discovered, which are: 7-4, 8-1, 8-3, 8-8, 8-9, 8-10, 8-11, 9-1, 9-2, 9-4, 10-1, and 10-2. It has been found that to get reliable results, one has to use a soft Mo pseudopotential in which $4s^2 4p^6$ electrons are represented explicitly and included into the valence shell; results obtained with a hard pseudopotential are misleading.

Generally, the low energy clusters are found to possess some symmetry ranging from C_s to T_d ; note, however, that most of the clusters have low symmetry like C_2 or C_s . We have also found that in many cases there are clusters of almost identical geometries and energies; however, their multiplicity is rather different and hence their electronic structure. In all cases there are at least a

few clusters of almost identical energy; this is important to take into account, e.g., when interpreting experiments [38] in which monoatomic clusters are produced with a fixed number of atoms, as there will be a distribution of clusters of different geometry and magnetic moment in the beam. Our free energy calculations also revealed that the order of clusters' stability may depend on temperature in a few cases. These findings display the intricate nature of cluster configurations and their energetic landscape. The interplay between spin multiplicity, bond lengths, and energies adds complexity to the understanding of these nanoscale systems.

We have also reported spin densities of all clusters with non-zero unpaired electrons. Interestingly, in three clusters with multiplicity $M = 1$ the spin density is also non-zero with positive and negative regions distributed equally within the cluster space.

We hope that the present study demonstrates an intriguing interplay of spin, symmetry, and electronic properties, that would be useful for researchers interested in physics of nanoparticles to uncover valuable insights into the fundamental principles governing these systems. This understanding holds promise for the development of novel materials, catalysts, and technologies that leverage the unique characteristics of nanoscale structures.

ACKNOWLEDGEMENTS

Y.W. is grateful for the funding from China Scholarship Council. The calculation is supported by UK's HEC Materials Chemistry Consortium, which is funded by EPSRC (EP/L000202), this work used the UK Materials and Molecular Modelling Hub for computational resources, MMM Hub, which is partially funded by EPSRC (EP/T022213/1, EP/W032260/1 and EP/P020194/1).

-
- [1] Penghui Shao, Ziwen Chang, Min Li, Xiang Lu, Wenli Jiang, Kai Zhang, Xubiao Luo, and Liming Yang. Mixed-valence molybdenum oxide as a recyclable sorbent for silver removal and recovery from wastewater. *Nature Communications*, 14(1):1365, 2023.
 - [2] Lei Yu, Wen-Gang Cui, Qiang Zhang, Zhuo-Fei Li, Yan Shen, and Tong-Liang Hu. Atomic layer deposition of nano-scale molybdenum sulfide within a metal-organic framework for highly efficient hydrodesulfurization. *Materials Advances*, 2(4):1294–1301, 2021.
 - [3] Melis S Duyar, Charlie Tsai, Jonathan L Snider, Joseph A Singh, Alessandro Gallo, Jong Suk Yoo, Andrew J Medford, Frank Abild-Pedersen, Felix Studt, Jakob Kibsgaard, et al. A highly active molybdenum phosphide catalyst for methanol synthesis from co and co₂. *Angewandte Chemie International Edition*, 57(46):15045–15050, 2018.
 - [4] Ryoichi Kojima and Ken-ichi Aika. Molybdenum nitride and carbide catalysts for ammonia synthesis. *Applied Catalysis A: General*, 219(1-2):141–147, 2001.
 - [5] Sharon J Nieter Burgmayer, Dori L Pearsall, Shannon M Blaney, Eva M Moore, and Calies Sauk-Schubert. Redox reactions of the pyranopterin system of the molybdenum cofactor. *JBIC Journal of Biological Inorganic Chemistry*, 9:59–66, 2004.
 - [6] Mao Miao, Jing Pan, Ting He, Ya Yan, Bao Yu Xia, and Xin Wang. Molybdenum carbide-based electrocatalysts for hydrogen evolution reaction. *Chemistry—A European Journal*, 23(46):10947–10961, 2017.
 - [7] Wenqin Zhang, Xiaorong Ran, Haitao Zhao, and Lichang Wang. The nonmetallicity of molybdenum clusters. *The Journal of chemical physics*, 121(16):7717–7724, 2004.
 - [8] Yue-Hong Yin and Jing Chen. The structures and properties of mon ($n = 2 - 15$) cluster. *Computational and Theoretical Chemistry*, 1212:113720, 2022.
 - [9] F Aguilera-Granja, A Vega, and LJ Gallego. A density-functional study of the structures, binding energies and magnetic moments of the clusters mon ($n = 2 - 13$), mo12fe, mo12co and mo12ni. *Nanotechnology*, 19(14):145704, 2008.

- [10] M Ziane, F Amitouche, S Bouarab, and A Vega. Density functional study of the structural, electronic, and magnetic properties of mo n and mo n s (n= 1- 10) clusters. *Journal of Nanoparticle Research*, 19:1–15, 2017.
- [11] Yue-Hong Yin and Jing Chen. Two quasi-degenerate isomers of mo13. *Journal of Cluster Science*, pages 1–11, 2023.
- [12] Byeong June Min. Study of the electronic and the structural properties of small molybdenum clusters via projector augmented wave pseudopotential calculations. *Journal of the Korean Physical Society*, 66:209–213, 2015.
- [13] Lei Xue-Ling. Theoretical study of small mo clusters and molecular nitrogen adsorption on mo clusters. *Chinese Physics B*, 19(10):107103, 2010.
- [14] Julián Del Plá and Reinaldo Pis Diez. Unraveling the apparent dimerization tendency in small mo n clusters with n= 3–10. *The Journal of Physical Chemistry C*, 120(39):22750–22755, 2016.
- [15] Faustino Aguilera Granja and Reinaldo Pis Diez. A density functional study of the interaction of dihydrogen with mon clusters (n= 2–8). adsorption and dissociation of h2 and cluster reconstruction after desorption. *International Journal of Quantum Chemistry*, 111(12):3201–3211, 2011.
- [16] Anderson S Chaves, Maurício J Piotrowski, and Juarez LF Da Silva. Evolution of the structural, energetic, and electronic properties of the 3d, 4d, and 5d transition-metal clusters (30 tm n systems for n= 2–15): A density functional theory investigation. *Physical Chemistry Chemical Physics*, 19(23):15484–15502, 2017.
- [17] Aslihan Sumer and Julius Jellinek. Computational studies of structural, energetic, and electronic properties of pure pt and mo and mixed pt/mo clusters: Comparative analysis of characteristics and trends. *The Journal of Chemical Physics*, 157(3):034301, 2022.
- [18] Zhe Ji, Christopher Trickett, Xiaokun Pei, and Omar M Yaghi. Linking molybdenum–sulfur clusters for electrocatalytic hydrogen evolution. *Journal of the American Chemical Society*, 140(42):13618–13622, 2018.
- [19] Subodh Kumar, Om P Khatri, Stéphane Cordier, Rabah Boukherroub, and Suman L Jain. Graphene oxide supported molybdenum cluster: first heterogenized homogeneous catalyst for the synthesis of dimethylcarbonate from co2 and methanol. *Chemistry—A European Journal*, 21(8):3488–3494, 2015.
- [20] Marta Feliz, Pedro Atienzar, Maria Amela-Cortés, Noée Dumait, Pierric Lemoine, Yann Molard, and Stéphane Cordier. Supramolecular anchoring of octahedral molybdenum clusters onto graphene and their synergies in photocatalytic water reduction. *Inorganic Chemistry*, 58(22):15443–15454, 2019.
- [21] N. Dugan and S. Erkoç. Genetic algorithms in application to the geometry optimization of nanoparticles. *Algorithms*, 2:410–428, 2009.
- [22] Chun-Sheng Liu, Ghanshyam Pilania, Chenchen Wang, and Ramamurthy Ramprasad. How critical are the van der waals interactions in polymer crystals? *The Journal of Physical Chemistry A*, 116(37):9347–9352, 2012.
- [23] Chris J Pickard and RJ Needs. High-pressure phases of silane. *Physical review letters*, 97(4):045504, 2006.
- [24] Chris J Pickard and RJ Needs. Ab initio random structure searching. *Journal of Physics: Condensed Matter*, 23(5):053201, 2011.
- [25] Georg Kresse and Jürgen Furthmüller. Efficient iterative schemes for ab initio total-energy calculations using a plane-wave basis set. *Physical review B*, 54(16):11169, 1996.
- [26] John P Perdew, Kieron Burke, and Matthias Ernzerhof. Generalized gradient approximation made simple. *Physical review letters*, 77(18):3865, 1996.
- [27] Stefan Grimme, Jens Antony, Stephan Ehrlich, and Helge Krieg. A consistent and accurate ab initio parametrization of density functional dispersion correction (dft-d) for the 94 elements h-pu. *The Journal of chemical physics*, 132(15), 2010.
- [28] Stefan Grimme, Stephan Ehrlich, and Lars Goerigk. Effect of the damping function in dispersion corrected density functional theory. *Journal of computational chemistry*, 32(7):1456–1465, 2011.
- [29] Georg Kresse and Daniel Joubert. From ultrasoft pseudopotentials to the projector augmented-wave method. *Physical review b*, 59(3):1758, 1999.
- [30] Yu M Efremov, AN Samoilova, VB Kozhukhovskiy, and LV Gurvich. On the electronic spectrum of the mo2 molecule observed after flash photolysis of mo (co) 6. *Journal of Molecular Spectroscopy*, 73(3):430–440, 1978.
- [31] John B Hopkins, Patrick RR Langridge-Smith, Michael D Morse, and Richard E Smalley. Supersonic metal cluster beams of refractory metals: Spectral investigations of ultracold mo2. *The Journal of Chemical Physics*, 78(4):1627–1637, 1983.
- [32] Benoit Simard, Marie-Ange Lebeault-Dorget, Adrian Marijnissen, and JJ Ter Meulen. Photoionization spectroscopy of dichromium and dimolybdenum: Ionization potentials and bond energies. *The Journal of chemical physics*, 108(23):9668–9674, 1998.
- [33] Vei Wang, Nan Xu, Jin-Cheng Liu, Gang Tang, and Wentong Geng. Vaspkit: A user-friendly interface facilitating high-throughput computing and analysis using vasp code. *Computer Physics Communications*, 267:108033, 2021.
- [34] Koichi Momma and Fujio Izumi. Vesta 3 for three-dimensional visualization of crystal, volumetric and morphology data. *Journal of applied crystallography*, 44(6):1272–1276, 2011.
- [35] Lev Kantorovich. *Quantum theory of the solid state: an introduction*, volume 136. Springer Science & Business Media, 2004.
- [36] Peter J Yunker, Ke Chen, Zexin Zhang, Wouter G Ellenbroek, Andrea J Liu, and Arjun G Yodh. Rotational and translational phonon modes in glasses composed of ellipsoidal particles. *Physical Review E*, 83(1):011403, 2011.
- [37] Elsa Passaro Snehal Kumbhar. Interactive phonon visualizer tool, 2023.
- [38] Federico Loi, Monica Pozzo, Luca Sbuelz, Luca Bignardi, Paolo Lacovig, Ezequiel Tosi, Silvano Lizzit, Aras Kartouzian, Ueli Heiz, Dario Alfè, et al. Oxidation at the sub-nanoscale: oxygen adsorption on graphene-supported size-selected ag clusters. *Journal of Materials Chemistry A*, 10(27):14594–14603, 2022.